Photophysical properties of cyclopalladates must be recognized in order to realize application of such systems in photoconversion roles. We have reported here initial photophysical studies of several ortho-metalated palladium compounds. Drawing from these results, we are actively modeling and studying additional palladium compounds that may be useful in the processes of energy or electron transfer.

Acknowledgment. This work was supported by the Office of Basic Energy Sciences, United States Department of Energy, Project DE-FG03-88ER13842. We wish to thank Fred Garces for obtaining the ^1H NMR spectral results.

Registry No. I, 20832-86-4; II, 117939-93-2; III, 117958-64-2; IV, 117939-94-3; ppy, 1008-89-5; [Pd(ppy)(en)]BF_4, 117939-96-5; Li_2PdCl_4, 15525-45-8.

Contribution from the Department of Chemistry, University of Alabama at Birmingham,
University Station 219 PHS, Birmingham, Alabama 35294, and Institut für Organische Chemie
der Friedrich-Alexander Universität Erlangen-Nürnberg, D-8520 Erlangen, Federal Republic of Germany

Remarkable Structures of Dialane(4), Al_2H_4

Koop Lammertsma,*[†] Osman F. Güner,[†] R. Michelle Drewes,[†] Alan E. Reed,[‡]
and Paul von Ragué Schleyer[‡]

Received December 8, 1987

The potential energy surface of dialane(4), Al_2H_4, has been studied by ab initio molecular orbital theory at the MP4(SDTQ)/6-31G**//HF/6-31G* + ZPE level. Five minima (**1**, **2**, **5**, **7**, and **8**) and three transition structures (**3**, **6**, and **9**) were determined at the HF/6-31G* level. The most stable isomers are salt-like structures: i.e., **1** (C_{3v}), being the face complex of Al^+ with tetrahedral AlH_4^-, and the 1.0 kcal/mol less stable **2** (C_{2v}), where Al^+ complexes to an AlH_4^- edge. Structure **5** (D_{2d}) is 10.7 kcal/mol less stable than **1**, with a barrier for Al–Al bond rotation of only 1.8 kcal/mol (**6**), and has an energy difference with **7** (H_3AlAlH) of 11.3 kcal/mol; the μ-hydrido structure **8** is of intermediate energy. The doubly hydrogen-bridged isomer **9** is the energetically least favored (transition) structure, in strong contrast to B_2H_4, where it represents a minimum with nearly the same energy as the D_{2d} isomer.

Introduction

Diverse structures can be exhibited by Al_2H_4 molecules with 10 valence electrons. The qualitative prediction, based on Walsh diagrams, that perpendicular $H_2A{-}AH_2$ geometries (D_{2d}) should be favored over planar arrangements (D_{2h}) has been verified by various theoretical calculations on B_2H_4.[1] Since experimentally known B_2X_4 (X = F, Cl, Br) molecules[2] prefer such classical geometries,[3] other structural possibilities have only been considered more recently. Initial examinations suggested B_2H_4 isomers with single and double hydrogen bridges as well with C_{3v} geometries not to be favorable. The same conclusion was reached in our study of the $C_2H_4^{2+}$ potential energy surface, where the usual D_{2d} $H_2C{-}CH_2^{2+}$ form was the global minimum.[4] However, $CH_3{-}B{-}H^+$ (C_{3v}) was the most stable CBH_4^+ isomer.[5] Moreover, very recent MINDO/3 calculations on $C_2H_4^{2+}$[6a] and ab initio results at correlated levels (MP2/6-31G**) for both $C_2H_4^{2+}$[6b] and B_2H_4[1a] showed doubly bridged geometries to be quite low in energy. Similar hydrogen-bridged (e.g., in $B_2H_7^-$,[7] $Al_2H_7^-$,[8] and $C_2H_n^+$[9]) and multiple-hydrogen-bridged arrangements (e.g., in Si_2H_2[10] but not in P_2H_2[11] or Si_2H_4[10b]) are now being found commonly.

Pertinent to the present work, Zakzhevskii and Charkin[12] included the salt-like structures $M^+[MCl_4]^-$ which are known for Ga_2Cl_4 and In_2Cl_4,[13] in their investigation of various M_2X_4 molecules (M = B, Al; X = H, F). With two different double ζ basis sets, they found Al_2H_4 to be quite unlike B_2H_4, which favors largely covalent structures. The salt-like $Al^+[AlH_4]^-$ isomer of the former was the most stable, although the $H_2Al{-}AlH_2$ (D_{2d} and D_{2h}) forms were close in energy.[12] These $Al^+[AlH_4]^+$ species are related to more conventional ionic molecules such as $M^+[AlH_4]^-$ and $M^+[BH_4]^-$ (M = Li,Na)[14] and $Li^+[CH_4]$,[15] and to species with "inverted" geometries,[16,17] e.g., $[SiH_3]^-Li^+$[16] and $[AlH_2]^-Li^+$[16] as well as carbon-based systems. The potential existence of Al_2H_4[18] and its relevance in Friedel–Crafts chemistry has been noted.[19]

Chart I

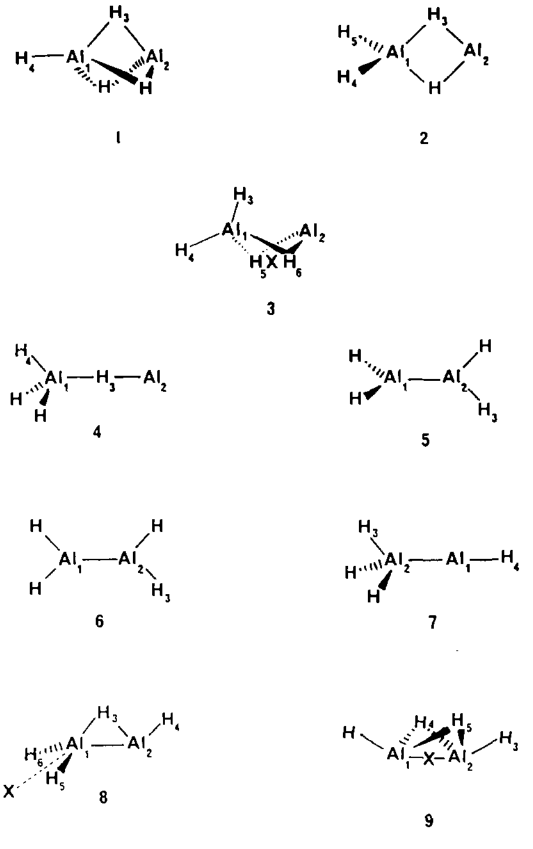

[†] University of Alabama at Birmingham.

[‡] Friedrich-Alexander Universität Erlangen-Nürnberg.

Table I. HF/6-31G* Optimized Al_2H_4 Geometries

	bond dist, Å			
geom	AlAl	Al_1H	Al_2H	bond angle, deg
HAl–H_3–Al (**1**, C_{3v})	2.5297	1.6716 (Al_1H_3) 1.5734 (Al_1H_4)	2.0227 (Al_2H_3)	
H_2Al–H_2–Al (**2**, C_{2v})	2.8053	1.7226 (Al_1H_3) 1.5843 (Al_1H_4)	1.8715 (Al_2H_3)	125.66 ($H_4Al_1H_5$)
HAl–H_3–Al (**3**, C_s)	2.5963	1.6204 (Al_1H_3) 1.5751 (Al_1H_4)	1.9296 (Al_2H_5) 2.2597 (H_5H_6)	63.37 ($H_3Al_1Al_2$) 129.22 ($H_3Al_1H_4$) 85.02 (Al_1XAl_2)
H_3Al–H–Al (**4**, C_{3v})	3.5507	1.8548 (Al_1H_3) 1.5985 (Al_1H_4)	1.6959 (Al_2H_3)	97.49 ($H_4Al_1Al_2$)
H_2Al–AlH_2 (**5**, D_{2d})	2.6127	1.5939 (Al_1H_3)		122.00 ($Al_1Al_2H_3$)
H_2Al–AlH_2 (**6**, D_{2h})	2.6282	1.5930 (Al_1H_3)		122.09 ($Al_1Al_2H_3$)
H_3Al–AlH (**7**, C_{3v})	2.8551	1.6131 (Al_1H_4)	1.5977 (Al_2H_3)	97.54 ($Al_1Al_2H_3$)
H_2Al–H–AlH (**8**, C_s)	2.5237	1.7133 (Al_1H_3) 1.5795 (Al_1H_5)	1.9796 (Al_2H_3) 1.5934 (Al_2H_4)	144.44 ($Al_1Al_2H_4$) 127.16 ($H_5Al_1H_6$) 162.10 (XAl_1Al_2)
HAl–H_2–AlH (**9**, C_{2v})	2.2273	1.7969 (Al_1H_4)	1.5647 (Al_2H_3)	166.13 ($Al_1Al_2H_3$) 101.24 (H_4XH_5)

Table II. Total (au) and Relative (kcal/mol) Energies of Al_2H_4 Isomers[a]

geom	HF/3-21G		HF/6-31G*		MP2FU/6-31G*		ZPE
HAl–H_3–Al (**1**, C_{3v})	−483.44076	0.0	−486.09132	0.0 (0)	−486.22213	0.0	18.3
H_2Al–H_2–Al (**2**, C_{2v})	−483.44727	−4.1	−486.09453	−2.0 (0)	−486.21981	1.5	18.3
HAl–H_3–Al (**3**, C_s)	−483.44068	0.1	−486.09047	0.5 (1)			18.1
H_3Al–H–Al (**4**, C_{3v})	−483.43603	3.0	−486.07533	10.0 (2)	−486.19297	18.3	16.7
H_2Al–AlH_2 (**5**, D_{2d})	−483.44175	−0.6	−486.09202	−0.4 (0)	−486.20873	8.4	17.3
H_2Al–AlH_2 (**6**, D_{2h})	−483.43826	1.6	−486.08961	1.1 (1)	−486.20589	10.2	17.0
H_3Al–AlH (**7**, C_{3v})	−483.42419	10.4	−486.06940	13.8 (0)	−486.18799	21.4	16.7
H_2Al–H–AlH (**8**, C_s)	−483.42133	12.2	−486.06994	13.4 (0)	−486.19493	17.1	17.2
HAl–H_2–AlH (**9**, C_{2v})	−483.39662	27.7	−486.05088	25.4 (1)	−486.18737	24.1	17.4

[a] The first numerical value at each level is the absolute energy; the second is the relative energy. Values in parentheses indicate the number of imaginary harmonic frequencies. ZPE is the zero-point energy.

Table III. Total (au) and Relative (kcal/mol) 6-31G** Energies of Al_2H_4 Isomers[a]

geom	HF		MP2		MP3		MP4		cor[b]
HAl–H_3–Al (**1**, C_{3v})	−486.09570	0.0	−486.23419	0.0	−486.26298	0.0	−486.27219	0.0	0.0
H_2Al–H_2–Al (**2**, C_{2v})	−486.09875	−1.9	−486.23222	1.2	−486.26148	0.9	−486.27059	1.0	0.9
HAl–H_3–Al (**3**, C_s)	−486.09473	0.6	−486.23119	1.9	−486.26014	1.8	−486.26934	1.8	1.6
H_2Al–AlH_2 (**5**, D_{2d})	−486.09547	0.1	−486.21905	9.5	−486.24574	10.8	−486.25357	11.7	10.5
H_2Al–AlH_2 (**6**, D_{2h})	−486.09306	1.7	−486.21630	11.2	−486.24295	12.6	−486.25073	13.5	12.2
H_3Al–AlH (**7**, C_{3v})	−486.07285	14.3	−486.19846	22.4	−486.22636	23.0	−486.23484	23.4	21.1
H_2Al–H–AlH (**8**, C_s)	−486.07390	13.7	−486.20551	18.0	−486.23353	18.5	−486.24243	18.7	16.8
HAl–H_2–AlH (**9**, C_{2v})	−486.05529	25.4	−486.19409	25.2	−486.22148	26.0	−486.23048	26.2	23.6
Al^{+}[c] (K_h)	−241.65276		−241.67873		−241.68713		−241.69010		
AlH[c] ($C_{\infty v}$)	−242.43878		−242.48709		−242.50019		−242.50480		
AlH_2[c] (C_{2v})	−243.01128		−243.06315		−243.07494		−243.07849		
AlH_3[c] (D_{3h})	−243.61899		−243.69031		−243.70554		−243.70971		
AlH_4^- (T_d)	−244.21622		−244.31050		−244.32991		−244.33536		

[a] The first numerical value at each level is the absolute energy; the second is the relative energy. [b] Scaled (0.9) ZPE corrected relative energies for MP4/6-31G**. [c] Reference 31.

Our goal was to examine the Al_2H_4 potential energy surface more fully at higher levels of ab initio theory.[20] Not only **1–6** but also singly and doubly hydrogen bridged structures and C_{3v} geometries (**7–9**) were included and characterized (see Chart I

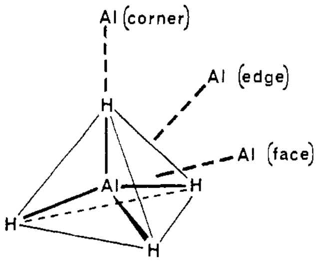

Figure 1. Face, edge, and corner complexation of Al^+ to the AlH_4^- tetrahedron.

---

(1) (a) Mohr, R. R.; Lipscomb, W. N. *Inorg. Chem.* **1986**, *25*, 1053. (b) Vincent, M. A.; Schaefer, H. F., III. *J. Am. Chem. Soc.* **1981**, *103*, 5677. (c) McKee, M. L.; Lipscomb, W. N. *Ibid.* **1981**, *103*, 4673. (d) Dill, J. D.; Schleyer, P. v. R.; Pople, J. A. *Ibid.* **1975**, *97*, 3402.

(2) (a) Danielson, D. D.; Hedberg, K. *J. Am. Chem. Soc.* **1979**, *101*, 3199. (b) Danielson, D. D.; Patton, J. V.; Hedberg, K. *Ibid.* **1977**, *99*, 6484. (c) Durig, J. R.; Thompson, J. W.; Witt, J. D.; Odom, J. D. *J. Chem. Phys.* **1973**, *58*, 5339. (d) Odom, J. D.; Saunders, J. E.; Durig, J. R. *Ibid.* **1972**, *56*, 1643. (e) Ryan, R. R.; Hedberg, K. *Ibid.* **1969**, *50*, 4986. (f) Atoji, M.; Wheatley, P. J.; Lipscomb, W. N. *Ibid.* **1957**, *27*, 196. (g) Trafanos, L.; Lipscomb, W. N. *Ibid.* **1958**, *28*, 54.

(3) Clark, T.; Schleyer, P. v. R. *J. Comput. Chem.* **1981**, *2*, 20.

(4) Lammertsma, K.; Barzaghi, M.; Olah, G. A.; Pople, J. A.; Kos, A. J.; Schleyer, P. v. R. *J. Am. Chem. Soc.* **1983**, *105*, 5252.

(5) Pople, J. A.; Apeloig, Y.; Schleyer, P. v. R. *Chem. Phys. Lett.* **1982**, *85*, 489.

(6) (a) Dewar, M. J. S.; Reynolds, C. H. *J. Mol. Struct.* **1986**, *136*, 209. (b) Nobes, R. N.; Wong, M. W.; Radom, L. *Chem. Phys. Lett.* **1987**, *136*, 299. Wong, M. W.; Yates, B. F.; Radom, L. *J. Am. Chem. Soc.* **1987**, *109*, 3181.

(7) (a) Raghavachari, K.; Schleyer, P. v. R.; Spitznagel, G. W. *J. Am. Chem. Soc.* **1983**, *105*, 5917. (b) Shore, S. G.; Lawrence, S. H.; Watkins, M. I.; Bau, R. *Ibid.* **1982**, *104*, 7669.

Table IV. 6-31G* Harmonic Frequencies (cm^{-1}) of Al_2H_4 Isomers

geom	
HAl–H_3–Al (**1**, C_{3v})	299 (e), 395 (a_1), 840 (e), 962 (e), 1008 (a_1), 1652 (e), 1800 (a_1), 2060 (a_1)
H_2Al–H_2–Al (**2**, C_{2v})	173 (b_1), 339 (a_1), 504 (b_2), 709 (a_2), 783 (a_1), 873 (b_1), 1123 (b_2), 1269 (a_1), 1346 (b_2), 1644 (a_1), 2015 (a_1), 2021 (b_1)
HAl–H_3–Al (**3**, C_s)	404 (a″), 413 (a′), 756 (a′), 843 (a″), 975 (a′), 992 (a″), 1103 (a′), 1519 (a″), 1679 (a′), 1889 (a′), 2054 (a′), 208 (a′) [i][a]
H_3Al–H–Al (**4**, C_{3v})	214 (a_1), 686 (e), 756 (a_1), 831 (e), 1813 (a_1), 1949 (e), 1985 (a_1), 155 (e) [i]
H_2Al–AlH_2 (**5**, D_{2d})	140 (b_1), 344 (e), 363 (a_1), 591 (e), 811 (b_2), 875 (a_1), 1969 (b_2), 1981 (e), 1993 (a_1)
H_2Al–AlH_2 (**6**, D_{2h})	310 (b_{2u}), 362 (a_g), 489 (b_{3u}), 510 (b_{3g}), 610 (b_{2g}), 815 (b_{1u}), 875 (a_g), 1973 (b_{1u}), 1980 (b_{3g}), 1988 (b_{2u}), 1997 (a_g), 139 (a_1) [i]
H_3Al–AlH (**7**, C_{3v})	182 (a_1), 191 (e), 467 (e), 745 (a_1), 816 (e), 1916 (a_1), 1951 (e), 1970 (a_1)
H_2Al–H–AlH (**8**, C_s)	223 (a′), 268 (a″), 455 (a″), 471 (a′), 508 (a′), 762 (a′), 776 (a″), 969 (a′), 1537 (a′), 1986 (a′), 2032 (a′), 2041 (a″)
HAl–H_2–AlH (**9**, C_{2v})	287 (a_2), 506 (a_1), 528 (b_1), 585 (a_1), 923 (a_2), 1021 (a_1), 1122 (b_2), 1485 (b_1), 1520 (a_1), 2091 (b_2), 2102 (a_1), 212 (b_2) [i]

[a] "i" denotes an imaginary frequency.

for structures).

Methods

Although initial ab initio calculations[21] using the Gaussian 82 program[22] were carried out with the smaller 3-21G basis set,[23] we report results on fully optimized (HF/6-31G*//HF/6-31G*)[24] geometries in Table I. This split-valence basis set is augmented by a set of six d functions on aluminum, which allow polarization. The 6-31G** basis set,[24] employed for single-point calculations to estimate the effect of valence electron correlation with the Møller-Plesset approximation at the full fourth order (MP4/6-31G**//HF/6-31G*),[25] also includes sets of p orbitals on each hydrogen. The relative energies of **1**–**9** at the HF/3-21G, HF/6-31G*, MP2(full)/6-31G*, HF/6-31G**, and MP_4/6-31G** levels, listed in Tables II and III along with the absolute energies, show the effects of basis set extension and of electron correlation to be significant. The final set of relative Al_2H_4 energies (in Table III) were obtained after correcting the MP4/6-31G** data for zero-point energy (ZPE) differences. These were based on 6-31G* frequencies and were scaled, as recommended, by 0.89.[21a,26] The 6-31G* frequency analysis (Table IV) revealed **1**, **2**, **5**, **7**, and **8** to be minima on the potential energy surface but **3**, **6**, and **9** to be transition structures, characterized by a single imaginary frequency. Structure **4** has two negative eigenvalues of the 6-31G* Hessian matrix. The charge distribution and bonding in the Al_2H_4 structures was studied by natural population analysis (NPA), employing natural bond orbitals (NBO), natural localized molecular orbitals (NLMO), and the HF/6-31G* wave functions.[27]

Results and Discussion

The various alane(4) structures investigated can be grouped into sets of isomers in which the Al–Al bonding is largely ionic in character and those that display covalent Al–Al bonding with or without hydrido bridging.

Ionic Structures. These structures involve tight interactions of an Al^+ cation with a tetrahedral AlH_4^- anion. Three combinations are feasible: Al^+ association to a face, edge, and corner of the AlH^- tetrahedron, as represented in Figure 1. The corresponding structures are **1**, **2**, and **4**. The ionic nature of these structures is confirmed by NPA, which shows that the charge on the "Al^+ cation" increases regularly from +0.63 in **1** to +0.71 in **2** to +0.85 in **4**. In each case, NBO analysis shows that the cationic aluminum has a single lone pair with occupancy 1.97–1.99 of dominant s character and that a charge transfer of roughly 0.15e from each adjacent Al–H bond of the AlH_4^- anion into the Al 3p orbitals occurs. The cationic aluminum is essentially unhybridized ($sp^{0.1}$ to $sp^{0.3}$), in contrast to the other, tetracoordinate aluminum, which displays significant hybridization ($sp^{1.4}$ to $sp^{1.6}$).[28] The smaller the number of donor Al–H bonds to the Al^+ cation, the larger the charges of the bridging hydrogens, which increase from –0.43 in **1** to –0.52 in **2** to –0.79 in **4**, revealing progressively increased polarization of the AlH_4^- anion by Al^+. Since the net charge on the Al^+ cation also increases along the series **1**, **2**, and **4**, the strength of ionic bonding between Al^+ and the proximate hydrogen(s) of AlH_4^- will strongly increase. As a result, the Al^+–H distances decrease from 2.023 Å in **1** to 1.871 Å in **2** to 1.696 Å in **4**, with corresponding increases in the AlH_4^- bonds pointing toward Al^+, from 1.573 Å in AlH_4^- to 1.672 Å in **1** to 1.723 Å in **2** to 1.855 Å in **4**. We now discuss specific features of these three structures.

The global energy minimum **1** has a densely packed structure with a surprisingly short Al–Al separation of 2.530 Å. This is even 0.083 Å less than that in the Al–Al single-bonded structure **5**. For comparison, the Al–Al bond length in metallic aluminum is 2.863 Å.[29] The interaction of the Al^+ cation with the three

---

(8) Howell, J. M.; Sapse, A. M.; Singman, E.; Synder, G. *J. Am. Chem. Soc.* **1982**, *104*, 4758. For $Al_2Cl_7^-$ see: Davis, L. P.; Dymek, C. J., Jr.; Steward, J. J. P.; Clark, H. P.; Lauderdale, W. J. *Ibid.* **1985**, *107*, 5041.

(9) $C_2H_3^+$, $C_2H_5^+$, and $C_2H_7^+$: Raghavachari, K.; Whiteside, R. A.; Pople, J. A.; Schleyer, P. v. R. *J. Am. Chem. Soc.* **1981**, *103*, 5649 and references cited therein.

(10) (a) Binkley, J. S. *J. Am. Chem. Soc.* **1984**, *106*, 603. (b) Luke, B. T.; Pople, J. A.; Krogh-Jespersen, M.-B.; Apeloig, Y.; Karni, M.; Chandrasekhar, J.; Schleyer, P. v. R. *Ibid.* **1986**, *108*, 270 and references cited therein.

(11) Allen, T. L.; Scheiner, A. C.; Yamaguchi, Y.; Schaefer, H. F., III. *J. Am. Chem. Soc.* **1986**, *108*, 7579.

(12) Zakzhevskii, V. G.; Charkin, O. P. *Chem. Phys. Lett.* **1982**, *90*, 117. Charkin, O. P. *The Stability and Structure of the Gaseous Inorganic Molecules, Radicals, and Ions*; Nauka: Moscow, 1980. For related studies of $Al_2H_3^+$ and its congeners, also see: Zyubin, A. S.; Charkin, O. P. *J. Struct. Chem.* (*Engl. Transl.*) **1987**, *27*, 882.

(13) Randloff, P. L.; Papatheodorou, G. N. *J. Chem. Phys.* **1980**, *72*, 992.

(14) Bonaccorsi, R.; Scrocco, E.; Tomasi, J. *Theor. Chim. Acta* **1979**, *52*, 113. For $MAlF_4$ (M = Li, Mg), see also: Curtiss, L. A. *Inorg. Chem.* **1982**, *21*, 400.; *Chem. Phys. Lett.* **1979**, *68*, 225.

(15) Schleyer, P. v. R.; Tidor, B.; Jemmis, E. D.; Chandrasekhar, J.; Würthwein, E.-U.; Kos, A. J.; Luke, B. T.; Pople, J. A. *J. Am. Chem. Soc.* **1983**, *105*, 484–491.

(16) (a) Schleyer, P. v. R.; Clark, T. *J. Chem. Soc., Chem. Commun.* **1986**, 1371. (b) Schleyer, P. v. R. to be submitted for publication.

(17) Charkin, O. P. *Theoretical Problems and Molecular Structure*; Zhanie: Moscow, 1987.

(18) Chai, B. J.; Ko, H. C.; Greenbaum, M. A.; Farber, M. *J. Phys. Chem.* **1967**, *71*, 3331.

(19) Hoberg, H.; Krause, S. *Angew. Chem., Int. Ed. Engl.* **1976**, *15*, 694. Olah, G. A. Personal communication.

(20) For an MNDO study on **2** and **4**, see: Baird, N. C. *Can. J. Chem.* **1985**, *63*, 71.

(21) For an introduction to the methods employed see: Hehre, W. J.; Radom, L.; Schleyer, P. v. R.; Pople, J. A. *Ab Initio Molecular Orbital Theory*; Wiley: New York, 1986.

(22) Binkley, J. S.; Frish, M. J.; Ragavachari, K.; DeFrees, D. J.; Schlegel, H. B.; Whiteside, R. A.; Fluder, E. M.; Seeger, R.; Pople, J. A. "Gaussian 82 (revision H)"; Carnegie-Mellon University: Pittsburgh, PA, 1984.

(23) Binkley, J. S.; Pople, J. A.; Hehre, W. J. *J. Am. Chem. Soc.* **1980**, *102*, 939. Gordon, M. S.; Binkley, J. S.; Pople, J. A.; Pietro, W. J.; Hehre, W. J. *Ibid.* **1982**, 104, 2797.

(24) Hariharan, P. C.; Pople, J. A. *Theor. Chim. Acta* **1973**, *28*, 213.

(25) Møller, C.; Plesset, M. S. *Phys. Rev.* **1934**, *46*, 618. Binkley, J. S.; Pople, J. A. *Int. J. Quantum Chem., Symp.* **1975**, *9*, 229. Pople, J. A.; Binkley, J. S.; Seeger, R. *Ibid.* **1976**, *10*, 1. Krishnan, R.; Pople, J. A. *Int. J. Quantum Chem.* **1978**, *14*, 91. Bartlett, R. J.; Purvis, G. D. *Int. J. Quantum Chem.* **1978**, *14*, 561. Wilson, S.; Saunders, V. R. *J. Phys.* **1979**, *B12*, 403. Krishnan, R.; Frish, M. J.; Pople, J. A. *J. Chem. Phys.* **1980**, *72*, 4244.

(26) The calculated harmonic frequencies are generally 11% too large; see ref 21 and: Pople, J. A.; Schlegel, H. B.; Krishnan, R.; DeFrees, D. J.; Binkley, J. S.; Frisch, M. J.; Whiteside, R. A.; Hout, R. F.; Hehre, W. J. *Int. J. Quantum Chem., Symp.* **1981**, *15*, 269.

(27) (a) Foster, J. P.; Weinhold, F. *J. Am. Chem. Soc.* **1980**, *102*, 7211. (b) Reed, A. E.; Weinstock, R. B.; Weinhold, F. *J. Chem. Phys.* **1985**, *83*, 735. (c) Reed, A. E.; Weinhold, F. *Ibid.* **1985**, *83*, 1736.

(28) These average atomic hybridizations are directly based on natural population analysis (s:p:d valence population ratios). They can also be derived from the hybridizations at each atom in the localized molecular orbitals; the hybrids in the LMOs are not restricted to be orthogonal, which has the consequence that geometric constraints do not force, for instance, sp^2 hybridization in AlH_3 and sp^3 hybridization in AlH_4^-. See: Reed, A. E.; Schleyer, P. v. R. *J. Am. Chem. Soc.* **1987**, *109*, 7362.

(face) hydrogens of $\mathrm{AlH_4^-}$ in **1** results in reduction of the ($\mathrm{Al{-}H_3}$) cone angle to 52.9° (in a perfect tetrahedron the cone angle from its center to a face is 70.5°; see Figure 1). As noted above, the three $\mathrm{Al^+{-}H}$ distances are 0.351 Å longer than the corresponding Al–H bonds of the $\mathrm{AlH_4^-}$ part, which in turn are only 0.099 Å longer than the fourth noninteracting Al–H bond, all in line with the ionic nature of **1**.

The Al–Al distance of 2.805 Å (HF/6-31G*) in the edge-complexed structure **2** is 0.275 Å longer than in the face-complexed **1**, which is expected for a less densely packed species. The strong reduction of the $\mathrm{AlH_4^-}$ tetrahedral angle HAlH for the two edge (or bridging) hydrogens to 81.3° (from an ideal 109.5°) is indicative of the sizable interaction with $\mathrm{Al^+}$. The HAlH angle involving the noninteracting hydrogens in the $\mathrm{AlH_4^-}$ unit expands to 125.7°. Because of the close relationship between **1** and **2**, a conversion between these two HF/6-31G* equilibrium structures was anticipated. Indeed, such a transition structure, **3**, was located. Since electron correlation effects strongly influence the $\mathrm{Al_2H_4}$ relative energies, we also optimized the higher energy isomer **2** at the MP2/6-31G* level and confirmed **2** to be an equilibrium structure at this level.[30]

In the $\mathrm{Al^+}$ corner-complexed $\mathrm{AlH_4^-}$ structure **4**, the polarization is so strong that the bridging hydrogen has as little covalent bonding to the "$\mathrm{AlH_4^-}$" aluminum as to the $\mathrm{Al^+}$ aluminum. The localized molecular orbital (NLMO) for the interacting Al–H bond has 5% contribution from both the $\mathrm{AlH_4^-}$ and $\mathrm{Al^+}$ aluminum atoms, with the remaining 84% from the hydrogen. The best description of the bonding would thus be $\mathrm{H_3Al_1{\cdots}H_3^-{\cdots}Al_2^+}$; the natural charges on $\mathrm{H_3Al}$, $\mathrm{H^-}$, and $\mathrm{Al^+}$ are −0.15, −0.70, and +0.85, respectively. The difference between bonds of the bridging hydrogen with the two Al atoms is more apparent when the hybridizations in the Al–H–Al NLMO are considered, which are $\mathrm{sp^{2.9}}$ at the $\mathrm{AlH_4^-}$ aluminum but $\mathrm{sp^{13}d^{0.6}}$ (89% p) at the $\mathrm{Al^+}$ aluminum. In light of this charge distribution and the nature of the two-electron, three-center Al–H–Al bond, it is not surprising that the interacting $\mathrm{Al_1{\cdots}H_3^-}$ bond is 0.159 Å *longer* than the $\mathrm{H_3^-{\cdots}Al_2^+}$ bond. The normal mode of the degenerate imaginary 6-31G* frequency for **4** suggests conversion to the more stable **2**, which is the global minimum at this level. In essence, **4** may represent a higher order hydride transfer from AlH to $\mathrm{AlH_3}$.

Covalent Structures. Similar to the well-studied diborane(4)[1] and ethylene dication,[4,6] the most stable dialane(4) with Al–Al covalent bonding has D_{2d} symmetry. This equilibrium structure **5** has an Al–Al bond length of 2.613 Å. Rotation around this bond to the planar transition structure **6** (D_{2h}) results in a lengthening of only 0.016 Å. This indication that only a very small amount of hyperconjugation from the Al–H bonds into the empty p orbital of the other Al is present in **5** is also confirmed by NBO analysis: the Al–H bonds are polarized in the wrong direction (toward hydrogen) for this interaction to be effective, and the Al p orbitals are very diffuse. A much stronger effect has been calculated for such bond rotations (D_{2d}–D_{2h}) in the first-row diborane(4)[1a] and ethylene dication $\mathrm{C_2H_4^{2+}}$,[4,6] with bond elongations of 0.089 Å for the 1.653-Å B–B bond (MP2/6-31G**) and 0.155 Å for the 1.432-Å C–C bond (HF/6-31G*), respectively.

Structure **7** (C_{3v}) has an Al–Al bond length of 2.855 Å, which is significantly longer than that of **5** and is actually the longest of all isomers calculated, thereby suggesting a weak Al–Al interaction. This is supported by the AlAlH bond angle of 97.5°, showing that the $\mathrm{AlH_3}$ fragment deviates only 7.5° from planarity. Hence, structure **7** may be viewed as an ylide-type species, composed of :AlH (Lewis base) complexed to $\mathrm{AlH_3}$ (Lewis acid). Accordingly, the Al charges by NPA are +0.46 (:AlH) and −0.46 ($\mathrm{AlH_3}$), and the weak covalent Al–Al bond arises from an ylide-type donor–acceptor interaction. The donor–acceptor nature of the Al–Al bond is shown by its NLMO, which is mainly on the :AlH fragment (aluminum 75.0%) and has hybridizations at the :AlH and $\mathrm{AlH_3}$ aluminums of $\mathrm{sp^{0.21}\,d^{0.00}}$ and $\mathrm{sp^{3.18}\,d^{0.03}}$, respectively. This structure emphasizes the ability of alane(4) to form ionic complexes. Thus, while **7** is an HF/6-31G* equilibrium structure, this is not the case for the corresponding C_{3v} diborane(4),[1a] probably due to the lower polarizability and electropositivity of boron, whereas the related $\mathrm{C_2H_4^{2+}}$ dication (C_{3v}) is a local minimum only at MP2/6-31G*, albeit with a barrier for rearrangement of <1 kJ/mol.[31]

***μ*-Hydrido Structures.** Hydrogen bridging, which is common in covalent boranes and carbonium ions, also manifests itself in alanes. The two $\mathrm{Al_2H_4}$ structures **8** and **9** both possess bridging hydrogen(s) as well as covalent Al–Al bonding. Conceptually, structures **8** and **9**, like **7**, can be considered to be complexes of :AlH with $\mathrm{AlH_3}$. However, in contrast to the case for **7** complexes **8** and **9** also allow back-donation from the Al–H bonds of $\mathrm{AlH_3}$ to the empty π orbitals of :AlH. Accordingly, the natural charge of the :AlH unit decreases from +0.46 in **7** to +0.37 in **8** and +0.38 in **9**. There is in addition a steady increase in degree of average hybridization along the series **7**, **8**, and **9**: $\mathrm{sp^{1.62}d^{0.03}}$ to $\mathrm{sp^{1.67}d^{0.04}}$ to $\mathrm{sp^{1.78}d^{0.04}}$ at the "$\mathrm{AlH_3}$" aluminum and $\mathrm{sp^{0.32}d^{0.01}}$ to $\mathrm{sp^{0.67}d^{0.01}}$ to $\mathrm{sp^{1.78}d^{0.04}}$ at the ":AlH" aluminum, respectively. The alane ($\mathrm{AlH_3}$)–alene (:AlH) interaction is so large in **8** and **9** that a more suitable description involves Al–Al two-center and Al–H–Al three-center bonds instead of partially occupied aluminum lone pairs.

The mono-H-bridged isomer **8** is an HF/6-31G* equilibrium structure in contrast with the case for the analogous diborane(4), where no stationary point resembling **8** could be obtained; the corresponding $\mathrm{C_2H_4^{2+}}$ dication form is a transition structure. Compared with its $\mathrm{Al_2H_4}$ isomers, **8** has a short Al–Al bond length of 2.524 Å, shorter than in the covalently bonded **5** by 0.089 Å. Structure **8** is further characterized by the inverted geometry of its singly end-substituted aluminum and the 35.6° bending of its attached hydrogen. The 1.980-Å Al–H bond distance of this aluminum to the bridging hydrogen is 0.267 Å (!) longer than that to the second aluminum, which has its two remaining hydrogens bent in the opposite direction. These structural parameters are consistent with a model structure of **8** involving a complex between $\mathrm{AlH_3}$ and AlH with one of the empty π orbitals of AlH interacting with an Al–H bond of $\mathrm{AlH_3}$. Indeed, the localized molecular orbital (NLMO) corresponding to the three-center bond is 18% polarized toward the alane ("$\mathrm{AlH_3}$") aluminum, 72% toward the bridging hydrogen, and only 10% toward the alene (":AlH") aluminum. The bridging hydrogen being closer to the alene than to the alane Al must be due to strong alene Al–H ionic attraction. Even more revealing are the hybridizations at the two Al atoms in this NLMO:$\mathrm{sp^{3.0}d^{0.1}}$ at the alane Al but 95% p at the alene Al. The composition of the NLMO for the Al–Al bond yields further support for the $\mathrm{AlH_3}$–:AlH model, as it is 71% polarized toward a hybrid on the alene Al of 71% s character and only 28% polarized toward a hybrid on the alane Al of $\mathrm{sp^{2.9}}$ character.

The di-H-bridged structure **9** has by far the shortest Al–Al bond length, of 2.227 Å (!), of all the species; this is a reduction of 0.386 Å from the covalent Al–Al bond in **5**. Similarly, the doubly hydrogen-bridged diborane(4)[1a] and $\mathrm{C_2H_4^{2+}}$ structures[4,31] have short covalent bonds. The Al–H bridging bond lengths in **9** are 1.797 Å. Since H is more electronegative than Al, the best model for structure **9** would be a π complex between linear $\mathrm{Al_2H_2^{2+}}$ (which has no π electrons) and two $\mathrm{H^-}$ anions, which is consistent with the near-orthogonality (101.24°) of the bridging hydrogens. The localized molecular orbitals (NLMOs) for the two Al–H–Al three-center bonds are polarized 69% toward H and 16% toward an $\mathrm{sp^8d^{0.3}}$ hybrid on each Al. In contrast, the hybridizations at Al in the NLMOs for the Al–Al and Al–H bonds are $\mathrm{sp^{1.52}d^{0.01}}$ and $\mathrm{sp^{0.86}d^{0.02}}$, respectively. It is of interest to note that all hy-

---

(29) Weast, R. C., Ed.; *Handbook of Chemistry and Physics*, 64th ed.; CRC: Boca Raton, FL, 1983.

(30) Also a planar $\mathrm{H_2AlH_2Al}$ form was investigated, representing the complexation of $\mathrm{Al^+}$ to planar $\mathrm{AlH_4^-}$; see: Krogh-Jespersen, M.-B.; Chandrasekhar, J.; Würthwein, E.-U.; Collins, J. B.; Schleyer, P. v. R. *J. Am. Chem. Soc.* **1980**, *102*, 2263. However, this structure has two imaginary HF/6-31G* frequencies and was not further investigated.

(31) The **9**-like $\mathrm{B_2H_4}$ structure is a stable minimum at the HF/6-31G* level, just as at MP2/6-31G** (see ref 1a), with no negative eigenvalues of the Hessian matrix.

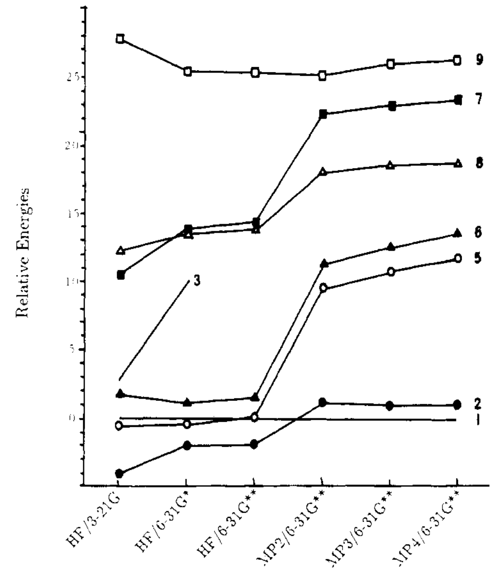

Figure 2. Plot of relative energies (in kcal/mol) vs basis set. All energies are relative to that of **1**.

drogens of **9** lie on one side of a plane through both aluminum atoms; the terminal hydrogens are bent by 13.9°! Hence, the aluminum atoms in **9** have inverted geometries, which are consistent with the rough AlH_3–:AlH donor–acceptor interaction model given above. Surprisingly, **9** is an HF/6-31G* transition structure, whereas the di-H-bridged B_2H_4 isomer is a minimum at this level[31] and is only 1.5 kcal/mol (MP2/6-31G**) less stable than the D_{2d} isomer.[1a] Even the corresponding $C_2H_4^{2+}$ structure is a high-energy minimum, albeit only at correlated levels (MP2/6-31G*).[32] Structure **9** seems to represent the transition structure for intramolecular H exchange between the aluminum atoms in **1**.

Energies. The global alane(4) minimum is the salt-like tridentate structure **1**. The energy difference between **1** and the other salt-like Al_2H_4 form, bidentate **2**, is only 1.0 kcal/mol (MP4/6-31G** + ZPE). At the same level, **1** is 10.7 kcal/mol more stable than the covalent structure **5**. The preference of dialane(4) for ionic structures is related to that of the corresponding ionic gallium and indium chlorides[13] and contrasts with that of diborane(4),[1a] which prefers covalent bonding. This is due to the very small electronegativity difference between B and H. Nevertheless, the covalent Al_2H_4 structures **5**, **7**, and **8** are local minima within only 25 kcal/mol of the global ionic minimum **1**. Also in contrast to the case for B_2H_4, where the di-H-bridged **9**-like structure is only 1.5 kcal/mol (MP2/6-31G**) less stable than the global D_{2d} minimum (**5**-like), the Al_2H_4 energy difference between **5** and **9** is 25.4 kcal/mol (MP4/6-31G* + ZPE), making **9** the energetically least favored form investigated. Moreover, the B_2H_4 isomers corresponding to the Al_2H_4 equilibrium structures **7** and **8** are not stationary points on the B_2H_4 potential energy surface.

Our "final" relative energies differ substantially from those reported by Zakzhevskii and Charkin.[12] Their study, which did not include structures **8** and **9** or frequency characterization of the stationary points, compares best with our 3-21G data. Electron correlation influences the relative Al_2H_4 energies to the greatest extent, in particular favoring the ion-pair structures **1** and **2**.[33] The effect of basis set extension is more subtle. Figure 2 illustrates these effects graphically.

The influence of electron correlation is most dramatic on the energy separation between ionic and covalent structures. For example, while the global minimum **1** is favored over **5** by 11.7 kcal/mol at the MP4/6-31G** level, this energy difference is marginal (0.1 kcal/mol) at the HF level and is −0.6 kcal/mol at HF/3-21G. Smaller energy variations are found between ionic and μ-hydrido isomers. Thus, while **1** is favored over **8** by 13.7 (12.2) kcal/mol at the HF/6-31G** (HF/3-21G) level, the energy difference increases to 18.7 kcal/mol at MP4/6-31G**. On the other hand, the energy difference between the di-H-bridged structure **9** and **1** remains nearly constant, i.e., within 25.4–27.7 kcal/mol. Although the level-dependent energy fluctuations are relatively small within the sets of ionic and covalent structures, they can also be important. This is illustrated by **1** and **2**. Whereas bidentate **2** is the most stable structure at the HF/3-21G level, its 4.1 kcal/mol energy difference with tridentate **1** is reduced to 1.9 kcal/mol at HF/6-31G** and reversed at all post-Hartree-Fock levels; **1** is favored over **2** by 1 kcal/mol at MP4/6-31G**. Consequently, the barrier for the conversion of **1** → **2** is less sensitive to the theoretical level. At the HF/3-21G level this barrier is 0.1 kcal/mol, which increases to 1.8 kcal/mol at MP4/6-31G**.

The 1.5 kcal/mol barrier (MP4/6-31G** + ZPE) for Al–Al bond rotation in **5** (D_{2d}), represented by **6** (D_{2h}), is very small and is in accord with the small structural changes discussed above. For the corresponding diborane(4) this barrier is 21.6 kcal/mol at the MP2/6-31G** level,[1a] while the energy required for the similar (D_{2d}–D_{2h}) C–C bond rotation in the more compact ethylene dication ($C_2H_4^{2+}$) amounts to 28.1 kcal/mol (MP3/6-31G**).[4] The energy difference between the two covalent dialane(4) structures **5** (D_{2d}) and **7** (C_{3v}) of 11.2 kcal/mol (MP4/6-31G** + ZPE) is small compared to that in the corresponding ethylidene dication isomers and nearly independent of the level of theory.

Stabilities. Consideration of possible fragmentation modes renders insight into the complexation energies of various Al_2H_4 isomers. Of course, these modes are different for ionic and covalent species. The dissociation energy for structure **1** into its Al^+ and AlH_4^- fragments (154.8 kcal/mol) is strongly endothermic as expected Coulombically. In sharp contrast, dissociation of **1** into the neutral AlH and AlH_3 fragments is endothermic by only 36.2 kcal/mol. All dialane(4) structures are thermodynamically stable both toward this fragmentation and toward dissociation affording two molecules of AlH_2. Nevertheless, the binding energies for the structures **7** and **8**, which represent complexes between AlH and AlH_3, are only 12.8 and 17.5 kcal/mol, respectively, or less than 1 eV.

Acknowledgment. The generous provision of computing time and the cooperation of the UAB Rust Computing Center greatly facilitated the present investigation. Acknowledgment is made to the donors of the Petroleum Research Fund, administered by the American Chemical Society, and the Research Corp. for support of this work in Alabama and to the Deutsche Forschungsgemeinschaft, the Fonds der Chemischen Industrie, and the Convex Corp. for support of this work in Erlangen. We thank Professor J. A. Pople for making the Gaussian-82 (IBM version) and -86 (VAX version) programs available.

Registry No. Al_2H_4, 65227-17-0.

---

(32) Whiteside, R. A.; Frisch, M. J.; Pople, J. A. *The Carnegie-Mellon Quantum Chemistry Archive*, 3rd ed.; Carnegie-Mellon University: Pittsburgh, PA, 1983.

(33) A very recent study on a comprehensive set of binary association complexes of LiH, BeH_2, and BH_3 rigorously addressed the effects of inclusion of electron correlation correction at the HF/6-31G** level.